Published in final edited form as:

Cancer Res. 2021 April 01; 81(7): 1827–1839. doi:10.1158/0008-5472.CAN-20-3157.

Survivin Expression is Differentially Regulated by a Selective Crosstalk between Rbm38 and miRNAs let-7b or miR-203a

Christopher A. Lucchesi[1], **Jin Zhang**[1], **Buyong Ma**[2,3], **Ruth Nussinov**[2], **Xinbin Chen**[1,*]

[1]Comparative Oncology Laboratory, Schools of Veterinary Medicine and Medicine, University of California at Davis, Davis, CA;

[2]Basic Science Program, Leidos Biomedical Research, Inc., Laboratory of Cancer ImmunoMetabolism, National Cancer Institute, Frederick, Maryland 21702, USA;

[3]School of Pharmacy, Shanghai Jiao Tong University, 800 Dongchuan Road, Shanghai 200240, China

Abstract

RNA-binding motif 38 (Rbm38) is a member of a protein family with a highly conserved RNA-binding motif and has been shown to regulate mRNA processing, stability, and translation. Survivin is an essential modulator of apoptotic and non-apoptotic cell death as well as a stress responder. Survivin mRNA is the fourth most frequently overexpressed transcript in the human cancer transcriptome, and its aberrant expression is associated with chemo-/radioresistance and poor prognosis. In this study, we examined whether survivin expression is regulated by Rbm38. Rbm38 bound to survivin 3′-UTR and suppressed miRNA let-7b from binding to and degrading survivin mRNA, leading to increased survivin expression. Rbm38 interacted with argonaute-2 (Ago2) and facilitated miR-203a-mediated degradation of survivin mRNA, leading to decreased survivin expression. Due to the abundance of let-7b over miR-203a, Rbm38 ultimately increased survivin expression in HCT116 and MCF7 cells. Additionally, Ser-195 in Rbm38 interacted with Glu-73/−76 in Ago2, and that Pep8, an 8 amino acid peptide spanning the region of Ser-195 in Rbm38, blocked the Rbm38-Ago2 interaction and inhibited miR-203a-mediated mRNA degradation, leading to enhanced survivin expression. Furthermore, Pep8 cooperated with YM155, an inhibitor of survivin, to suppress tumor spheroid growth and viability. Pep8 sensitized tumor cells to YM155-induced DNA damage in an Rbm38-dependent manner. Together, our data indicate that Rbm38 is a dual regulator of survivin and that Pep8/YM155 may be therapeutically explored for tumor suppression.

Keywords

Rbm38; Ago2; Survivin

*Correspondence to: Xinbin Chen xbchen@ucdavis.edu, University of California, Davis, Comparative Oncology Laboratory, 2128 Tupper Hall, VM: Surgical and Radiological Sciences, Davis, CA, 95616, (530-754-8404).

The authors declare no conflict of interest.

Introduction

RNA-binding motif protein 38 (Rbm38) and Rbm24 constitute a family of RNA-binding proteins with a single RNA-binding motif (1). Functionally, Rbm38 binds to mRNA targets, modulating mRNA processing, stability and/or translation thereby regulating an array of genes responsible for various cellular functions, including cellular growth and differentiation (2,3). Importantly, amplified Rbm38 expression has been correlated with the progression of colorectal adenoma to carcinoma and poor prognosis in multiple cancers, including breast cancer and lymphoma (2,4–6). We previously identified that Rbm38 suppresses p53 mRNA translation by interacting with eukaryotic translation initiation factor 4E (eIF4E) on p53 mRNA (2). Additionally, an 8 amino acid peptide derived from Rbm38 (Pep8), increases p53 translation by disrupting the Rbm38-eIF4E complex, leading to p53-dependent growth suppression *in vitro* and *in vivo* (7). Recently, we showed that Rbm38 works in concert with Argonaute-2 (Ago2) and miR-203a to regulate p63 expression (8). Moreover, Rbm38 can also regulate the accessibility of miRNAs on p21, Large Tumor Suppressor Kinase 2 (LATS2), and Sirtuin 1 (SIRT1) transcripts (9). These data suggest that Rbm38 alone, or together with various miRNAs can modulate an array of targets thereby influencing numerous biological functions.

microRNAs (miRNAs) have gained enormous interest giving their vast number and robust influence on mRNA stability and translation (10). Aberrant regulation of miRNA expression and function have been linked to many diseases, including diabetes and cancer (11). Compounding the importance of miRNAs, it is estimated that these small non-coding RNAs could influence more than 60% of all protein coding genes (12,13). A key component of miRNA-guided gene silencing is Ago2, which is also necessary for miRNA maturation. Ago2 is the only member of the AGO family that has a catalytic activity and plays an essential role within the RNA-induced silencing complex (RISC) (14,15). In a ribonucleo-protein complex, miRNAs bind to target mRNA 3′–untranslated regions (3′-UTR) and then guide the RISC via Ago2 to degrade target mRNAs (16,17).

Survivin is an essential modulator of cell death as well as a stress responder (18). Of clinical interest, survivin is the fourth most frequently overexpressed transcript in the human cancer transcriptome, and aberrant expression has been associated with chemo-/radio-resistance and poor prognosis (19,20). As Rbm38 and survivin are both overexpressed in tumors and promote tumor progression (19–22), we sought to address whether survivin is regulated by Rbm38, especially considering that survivin mRNA stability is known to be regulated by multiple miRNAs. Herein, we reported that Rbm38 regulates survivin mRNA stability via two distinct mechanisms. Rbm38 increases survivin expression by binding to a poly-U element in survivin 3′-UTR hindering the accessibility of let-7b. In contrast, Rbm38 decreases survivin expression by interacting with Ago2 and facilitating miR-203a-mediated degradation of survivin mRNA. Due to the abundance of let-7b over miR-203a in the cells tested in this study, Rbm38 ultimately enhances survivin expression. We demonstrated that Ser-195 in Rbm38 interacts with Glu-73 and/or Glu-76 in Ago2. Furthermore, Pep8 is a potent inducer of survivin by blocking Rbm38-Ago2 interaction, preventing miR-203a-mediated degradation of survivin mRNA. Last, we found that combinatorial administration of Pep8 and survivin inhibitor YM155 induces DNA damage in an Rbm38-dependent

manner, leading to enhanced growth suppression and decreased cell viability. Thus, concomitant administration of Pep8 and YM155 may be an effective therapeutic approach for cancers.

Materials and Methods

Cell lines

Cell lines HCT116 (ATCC Cat# CCL-247, RRID:CVCL_0291) and MCF7 (ATCC Cat# HTB-22, RRID:CVCL_0031) were obtained from ATCC between 2007 and 2016 and used below passage 25 or within 2 months after thawing. Since cell lines from ATCC have been thoroughly tested and authenticated, these cell lines were not re-authenticated or tested for mycoplasma. Cells were cultured in DMEM (Dulbecco's Modified Eagle's medium, Invitrogen, Carlsbad, CA) supplemented with 10% fetal bovine serum (Hyclone, Logan, UT, USA) and 100 U/mL penicillin/streptomycin in a humidified incubator with 5% CO_2 at 37° C. Generation of knockout and inducible cell lines are detailed in supplementary materials.

miRNA transfection

Micro-RNA transfections were performed using Lipofectamine RNAiMAX (Invitrogen, Carlsbad, CA) according to the manufacturer's instructions. Detailed methods and primers are listed in supplementary materials and supplementary table 1.

EGFP reporter assay with intact survivin 3′-UTR or poly-U deleted 3′-UTR

HCT116-Tet-On-Rbm38 cells were seeded (2×10^5 cells per well) on day 1. The next day, one well was transfected with 5 μg pCDNA3-EGFP-3′-UTR and the other with 5 μg pCDNA3-EGFP-3′-UTR-ΔpolyU. The following morning, each well was split equally into two new wells in a 6-well plate. That evening, one well of each duplicate was treated with 0.5 μg/mL tetracycline to induce Rbm38 expression. 18 hours later, cells were lysed and subjected to western blot analysis. All western blot figures are representative data of at least two independent replicates.

Pulldown assay with Biotin-tagged LNA of miRNA mimic

Biotin-based pulldown assay was adapted from Dash et al. (23). Detailed methods are listed in supplementary materials.

RNA isolation, RT-PCR, and quantitative RT-PCR

Total RNA was isolated with Quick-RNA Miniprep Kit (Zymo Research, Irvine, CA). cDNA was synthesized using RevertAid First Strand cDNA Synthesis kit (ThermoFisher Scientific). Detailed methods are listed in supplementary materials and primers in supplementary table 1.

Peptide synthesis and delivery

Peptides were synthesized by GenScript (Piscataway, NJ). Penetratin cell-penetrating peptide was used to facilitate intracellular delivery (24). Peptides used in this study are listed in supplementary table 2.

Western blot analysis, immunofluorescence, and immunoprecipitation-western blot analysis

Western blot procedures were as previously described (25). Detailed methods for immunofluorescence and immunoprecipitation (IP)-western blot analysis are listed in supplementary materials.

RNA-ChIP assay

For Rbm38 RNA-IP assays, Rbm38-inducuble MCF7 cells were seeded at 2 × 10^6 in four 10 cm plates. The next day, 2 plates were induced to express Rbm38 by addition of 100 ng/mL tetracycline for 36 hours followed by RNA-Chip assay as described previously (7). For Ago2 RNA-ChIP with Pep8 treatment, MCF7 cells were treated with 10 μM Pen-Control or Pen-Pep8 for 18 hours. Cell extracts were prepared with immunoprecipitation buffer (10 mM HEPES, pH 7.0, 100 mM KCl, 5 mM MgCl2, 0.5% Nonidet P-40, and 1 mM DTT) and then incubated with 1 μg of anti-Rbm38, anti-Ago2 or an isotype control IgG overnight at 4 °C. The RNA–protein immunocomplexes were brought down by magnetic protein A/G beads. Quantitative real-time PCR (qRT-PCR) for Rbm38 RNA-IP analysis and RT-PCR for Ago2 RNA-IP analysis were carried out to determine the levels of survivin and hypoxanthine phosphoribosyltransferase 1 (HPRT1) transcripts.

3D Spheroid Culture

3D “mini ring” spheroid culture assay was adapted from Phan et al., (26). Detailed methods are listed in supplementary materials.

Statistical analysis

All data were analyzed using Prism 8 (GraphPad). Experimental values were presented as mean ± SEM. Statistical comparisons between experimental groups were analyzed by a two-tailed Student’s t-test. P values < 0.05 were considered statistically significant.

Data availability

The authors declare that all data supporting the findings of this study are available within the article and its supplemental information files. Detailed Materials and Methods are given in supplementary materials. Research reagents will be provided upon a written request.

Results

Rbm38 increases survivin expression by hindering let-7b-mediated mRNA degradation

Utilizing the Xena Browser and the TCGA-Pan-Cancer database (27), we found that the expression level of survivin correlates with that of Rbm38 in various cancers (Suppl. Fig. 1A). Rbm38 and survivin are also known to be overexpressed in tumors and promote tumor progression (2,4–6). Additionally, survivin 3′-UTR contains a nonconical binding site for let-7b as well as an adjacent Rbm38-binding poly-U element (Fig. 1A) (28). As Rbm38 is capable of inhibiting miRNA binding to targets which contain an U-rich element (9), we examined whether survivin expression is regulated by Rbm38. We previously reported that Rbm38 negatively regulates p53 translation (2) and additionally, survivin and let-7b have

been shown to be transcriptionally repressed by p53 (29,30). Therefore, we examined the effect of Rbm38 on survivin expression in both p53-competent and p53-null HCT116 and MCF7 cells. We showed that let-7b inhibited survivin expression in a dose-dependent fashion (Figs. 1B–C), while Rbm38 enhanced survivin mRNA in both HCT116 and MCF7 cells independent of p53 (Figs. 1D–E, Suppl. Figs. 1B–C). Conversely, survivin expression was decreased in Rbm38-null cells (Fig. 1F, Suppl. Fig. 1D). Moreover, RNA-ChIP assay showed that the level of survivin mRNA was significantly higher in anti-Rbm38 immunoprecipitates from Rbm38-expressing cells than that from control cells (Suppl. Fig. 1E). Further, survivin mRNA half-life was decreased by loss of Rbm38 by almost half in Rbm38-null MCF7 cells (Suppl. Fig. 1F). These data suggest that Rbm38 is necessary to maintain survivin mRNA stability.

To determine if Rbm38 binding to survivin mRNA is necessary to regulate survivin expression, we generated two green fluorescent protein (GFP) reporter constructs in which GFP was coupled to either the full-length survivin 3′-UTR or the one with the poly-U element removed (Fig. 1G). Rbm38 increased the level of GFP protein with full-length 3′-UTR but had no effect on the level of GFP from the reporter carrying the poly-U deleted 3′-UTR (Fig. 1H). As an internal control, the level of endogenous survivin was still increased by Rbm38 expression (Fig. 1H). Since the binding sites for Rbm38 and let-7b are adjacent (Fig. 1A), we postulated that Rbm38 suppresses let-7b from binding to survivin mRNA. To test this, we examined the level of survivin mRNA and protein in p53-null HCT116 cells transfected with Rbm38 alone or together with let-7b. Expectedly, let-7b reduced, whereas Rbm38 increased, survivin expression (Fig. 1I, Suppl. Fig. 1G), whereas ectopic expression of Rbm38 restored the level of survivin mRNA and protein suppressed by let-7b (Fig. 1I, Suppl. Fig 1G). While let-7b had similar effects to regulate survivin in Rbm38-null cells as compared to isogenic control cells (Fig. 1J), we showed that Rbm38 suppressed let-7b degradation of survivin mRNA in a dose-dependent manner (Suppl. Fig. 1H). Furthermore, we measured the effect of a let-7b inhibitor and showed that the let-7b inhibitor was able to increase the level of survivin mRNA, albeit only weakly in Rbm38-competent cells (Fig. 1K, compare lanes 1–2), suggesting that the steady-state level of Rbm38 is sufficient to counter endogenous let-7b. In contrast, the let-7b inhibitor rescued survivin expression in Rbm38-null cells (Fig. 1K, compare lanes 3–4). To validate that Rbm38 suppresses the binding of let-7b to survivin mRNA, RNA pulldown assay was performed with biotin-tagged locked nucleic acid (LNA) of let-7b mimic. We showed that let-7b ability to interact with survivin mRNA was suppressed by Rbm38 in both MCF7 and HCT116 cells (Fig. 1L). Together, these data indicate that Rbm38 interacts with the poly-U element in survivin mRNA, thus positively regulating survivin expression by hindering let-7b-mediated mRNA degradation.

Rbm38 facilitates miR-203a-mediated degradation of survivin mRNA

miR-203a was found to regulate survivin via binding to a region distal to the poly-U element in survivin 3′-UTR (Fig. 2A) (31). Since Rbm38 decreases p63 mRNA stability via miR-203a by directly interacting with Ago2 (8), we postulated that Rbm38 may also regulate survivin via miR-203a. First, we confirmed that miR-203a was able to decrease survivin protein expression in wild type and p53-null HCT116 cells (Figs. 2B–C). We verified that the levels of survivin mRNA and protein were decreased by miR-203a but

increased by Rbm38 in p53-null HCT116 cells (Fig. 2D, Suppl. Fig. 2A). However, in the presence of miR-203a, Rbm38 was not able to rescue survivin mRNA (Fig. 2D, Suppl. Fig. 2A), suggesting that Rbm38 does not suppress miR-203a from targeting survivin mRNA as it does for let-7b. We also showed that Rbm38 enhanced miR-203a-mediated degradation of survivin mRNA in a dose-dependent manner (Suppl. Fig. 2B). Further, miR-203a had limited ability to suppress survivin expression in Rbm38-null cells as compared to isogenic control cells (Fig. 2E). Conversely, we found that miR-203a inhibitor was not able to enhance survivin expression in Rbm38-null cells (Fig. 2F).

The above studies suggest that Rbm38 has two opposing effects on survivin expression via let-7b and miR-203a. Since survivin expression is increased by ectopic expression of Rbm38 but decreased by knockout of Rbm38, we postulated that the relative abundance of these two miRNAs might be responsible for the dominant positive effect of Rbm38 on survivin expression. We preformed quantitative RT-PCR to measure the relative levels of miR-203a and let-7b. Indeed, we found that the levels of let-7b were several folds higher than that of miR-203a in both HCT116 and MCF7 cells (Fig. 2G). Together, our data indicate that Rbm38 regulates survivin expression via two opposing pathways: (1) the Rbm38-Ago2-miR-203a axis decreases the stability of survivin mRNA by promoting the formation of RISC complex; (2) Rbm38 enhances survivin mRNA stability by impinging let-7b accessibility.

The contact between Ser-195 in Rbm38 and Glu-73 and/or Glu-76 in Ago2 is critical for Rbm38-Ago2 interaction

Previously, we found that Rbm38 and Ago2 can be detected by co-immunoprecipitation (8). However, it remains uncertain whether Rbm38 and Ago2 interact with each other directly. To test this, recombinant full-length Ago2 protein and several Ago2 fragments were produced and used for immunoprecipitation (IP)-western blot analysis (Fig. 3A and Suppl. Fig. 3A). We showed that Rbm38 interacted with the full-length Ago2 and the N-terminal fragment (aa 1–227), but little if any with C-terminal fragments (aa 446–580 and aa 581–859) (Fig. 3B). Of note, the Ago2 fragment containing aa 228–445 failed to express, as such was unable to be tested. Additionally, we generated two small N-terminal fragments (aa 70–227 and aa 140–227) (Fig. 3A). We found that Rbm38 was able to interact with fragment aa 70–227 but not aa 140–227 (Fig. 3C), indicating that the region between aa 70–140 in Ago2 is necessary for its interaction with Rbm38.

We showed previously that Ser-195 phosphorylation inhibits Rbm38 ability to interact with eIF4E or Ago2 (8,32). We also found that Pep8, derived from aa 190–197 in Rbm38, including Ser-195, is capable of blocking the interaction between Rbm38 and eIF4E (7). Thus, we extrapolated that Pep8 may also block Rbm38 from binding to Ago2. To test this, IP-western blot analysis was performed and showed that the interaction between Rbm38 and Ago2 was inhibited by Pep8, supporting the idea that Rbm38 interacts with eIF4E or Ago2 via the same domain (Fig. 3D).

To define the critical contact residue(s) in Ago2 for its interaction with Rbm38, extensive molecular dynamic (MD) simulations were performed to determine the binding site on Ago2 for Pep8, and by extension for Rbm38. In the apo state of Ago2, a gating movement of the

PAZ domain was observed with the RNA binding grove completely opened after 4 microsecond simulation (Suppl. Figs. 3B–C). The overall root-mean-square deviation (RMSD) of the whole protein reached to 12 Å, mainly due to domain motions (Suppl. Fig. 3D). The distance between the PAZ and MID domains was measured by the Cα distance of Lys-263 in the PAZ domain and Asp-823 in the MID domain. Lys-263 and Asp-823 formed a salt bridge in the closed conformation but were separated by more than 50 Å in the open conformation (Suppl. Fig. 3E). There was a slight variation in the N-terminal domain structure in Ago2 between crystal structures 6n4o and 4f3t (33,34). In the 6n4o structure, a hydrogen bond was formed between Glu-76 and Tyr-393 (Suppl. Fig. 3B) whereas in the 4f3t structure, Glu-76 and Tyr-393 had no contact, indicating that there is a flexibility in the N-terminal domain. Additionally, the N-terminal domain still had a relatively large RMSD (3–6 Å) as compared with a rigid protein domain (Suppl. Fig. 3D). The distance between Glu-76 and Tyr-393 varied from a close contact with hydrogen bond formation to a separation of 20 Å.

To screen for possible docking sites for Pep8 around the N-terminal region, the protein docking program MEGADOCK was used (Fig. 3E) (35). We found that a hydrogen bond between Ser-6 in Pep8 and Glu-76 in Ago2 was the predominant binding mode (Fig. 3F, left panel). We also observed two alternative binding modes with slight variations represented by Ser-6 positioned between Glu-73 and Glu-76 (Fig. 3F, middle and right panels), suggesting that these negatively charged residues in Ago2 may be necessary for the interaction with Pep8.

To experimentally validate the model, we generated three N-terminal Ago2 fragments (aa 1–227) in which one or both negatively charged glutamic acid residues were substituted with a glutamine (Ago2 227-E73Q, Ago2 227-E76Q, and Ago2 227-E73Q/E76Q). IP-western blot analysis revealed that Ago2 227-E73Q and Ago2 227-E76Q were still capable of interacting with Rbm38, albeit at a lower affinity (Fig. 3G). In contrast, Ago2 227-E73Q/E76Q was unable to interact with Rbm38 (Fig. 3G). Additionally, we generated two Pep8 variants wherein Ser-6 was mutated to a negatively charged aspartic acid (Pep8SD) or a positively charged lysine (Pep8SK). Based on our modeling, mutating Ser-6 to a negatively charged aspartic acid would inhibit, whereas mutating to a positive charged lysine would enhance, the binding of Pep8 to the negatively charged pocket created between Glu-73 and Glu-76 in Ago2. A competitive GST pull-down assay was performed to measure the interaction of recombinant Ago2 with GST-tagged Rbm38 in the presence of a control (a scrambled 11-mer peptide: STLWDTAELWQ), Pep8, Pep8SD, or Pep8SK peptide. Indeed, we found that both Pep8 and Pep8SK were able to inhibit the binding between Rbm38 and Ago2 whereas Pep8SD had a much weaker effect (Fig. 3H). These data suggest that the negatively charged pocket created between Glu-73 and Glu-76 is likely the binding interface for Rbm38.

Pep8 promotes survivin expression by preventing Ago2-miR-203a from degrading survivin mRNA in an Rbm38-dependent manner

As an essential component of the RISC complex, Ago2 is recruited by miRNA to serve as a guide to load the RISC complex to target mRNA (16,17). Therefore, RNA-ChIP assay was performed and showed that Pep8 markedly inhibited Ago2 to interact with survivin mRNA

(Fig. 4A). Consistently, we found that Pep8 alone was able to increase survivin expression (Fig. 4B), and further, Pep8 cooperated with Rbm38 to markedly increase survivin mRNA (Fig. 4B). As p53 is known to decrease let-7b but increase miR-203 expression (30,36), we asked if increased expression of p53 by Pep8 (7) plays a role in survivin expression by Pep8. We found that survivin expression was increased by Pep8 in isogenic control and p53-null cells, but not in Rbm38-null cells (Suppl. Fig. 4), suggesting that the effect of Pep8 on survivin is Rbm38-dependent but p53-independent.

Previously, we showed that Ago2 interacts strongly with Rbm38-S195A, but weakly with Rbm38-S195D (8). Thus, we postulated that if the disruption of the Rbm38-Ago2 complex is necessary for Pep8 to regulate survivin expression, Pep8 would not have any effect on survivin in Rbm38-S195D expressing cells. Thus, we measured the effect of Pep8 on survivin in p53-null HCT116 cells uninduced or induced to express Rbm38-S195A or Rbm38-S195D. We found that survivin was increased similarly by Rbm38-S195A and Rbm38-S195D (Figs. 4C–D, compare lanes 1–2). These results are consistent with the idea that Rbm38-S195A and Rbm38-S195D, both of which are competent RNA-binding proteins (32), can bind to the poly-U element and prevent let-7b from degrading survivin mRNA. However, we found that survivin expression was further increased by Pep8 in Rbm38-S195A-expressing cells but little if any in Rbm38-S195D-expressing cells (Figs. 4C–D, compared lanes 3–4).

Next, we examined whether Pep8 increases survivin expression by preventing miR-203a or let-7b from degrading survivin mRNA. To test this, the effect of Pep8 on survivin was measured in p53-null HCT116 cells co-transfected with either miR-203a or let-7b. Expectedly, survivin mRNA was markedly reduced by miR-203a but increased by Pep8 (Fig. 4E). We showed that Pep8 was able to restore the level of survivin mRNA decreased by miR-203a (Fig. 4E, compare lane 2 with 4), suggesting that Pep8 is highly potent to prevent both exogenous and endogenous miR-203a from targeting survivin mRNA for degradation. Since Pep8 binds to Ago2 but not Rbm38, Pep8 should not influence the ability of Rbm38 to bind to the poly-U-rich element in survivin mRNA. Indeed, we found that Pep8 had little if any effect to reverse let-7b-mediated degradation of survivin mRNA (Figs. 4F, compare lane 2 with 4). Collectively, our data indicate that Pep8 blocks the interaction between Rbm38 and Ago2, thereby enhancing survivin mRNA stability by inhibiting miR-203a activity.

Pep8 sensitizes tumor spheroids to survivin inhibitor YM155 in an Rbm38-dependent manner

Previously, we demonstrated that Pep8 is a potent growth inhibitor of tumor xenografts in part by enhancing p53 expression (7). As survivin expression has been correlated with chemo-/radio-resistance and poor prognosis (20), increased expression of survivin by Pep8 could be detrimental therapeutically. Thus, we hypothesized that by abrogating Pep8-mediated induction of survivin we may further sensitize tumor cells to Pep8 treatment. Accordingly, we asked if YM155, a potent inhibitor of survivin transcription (37), could abrogate Pep8-mediated enhancement of survivin expression. To that end, wild type, Rbm38-null, and p53-null MCF7 and HCT116 cells were treated with Pep8, YM155, or in combination. Expectedly, YM155 inhibited survivin expression in all the cells tested (Figs.

5A–C and Suppl. Figs. 5A–C). Similarly, Pep8 enhanced survivin expression in both isogenic control and p53-null cells (Figs. 5A, 5C. Suppl. Figs. 5A and 5C), whereas Pep8 alone was able to enhance p53 expression in isogenic control cells (Fig. 5A and Suppl. Fig. 5A), consistent with our previous study (7). Importantly, YM155 was able to abrogate Pep8-induced survivin expression in both isogenic control and p53-null cells (Figs. 5A, 5C, Suppl. Figs. 5A and 5C, compare lane 2 with 4). Moreover, we found that Pep8 cooperated with YM155 to further enhance p53 induction (Fig. 5A and Suppl. Fig. 5A). In contrast, Pep8 had no effect on survivin or p53 expression in Rbm38-null cells (Fig. 5B and Suppl. Fig. 5B).

We next questioned if concomitant treatment with Pep8 and YM155 could suppress cell growth. To address this, MCF7 3D tumor spheroid cultures were used, which have been shown to more accurately mimic the main features of human solid tumors, thus more precisely recapitulating drug response (38). Pep8 treatment alone resulted in substantial growth suppression and decreased cell viability in isogenic control cells (Figs. 5D–E) but had minimal, if any, effect in cells deficient in Rbm38 or p53 (Figs. 5F–I), consistent with our early observations (7). Further, a low dose of YM155 (3 nM) had only a modest effect on MCF7 cells (Figs. 5D–E), which is consistent with a previous report that GI50 of YM155 for MCF cells is ~29 nM (39). Nevertheless, combined treatment with Pep8 and YM155 significantly decreased tumor spheroid growth and cell viability in isogenic MCF7 cells as compared to Pep8 or YM155 treatment alone (Fig. 5D–E). Intriguingly, while Rbm38-null MCF7 cells were not sensitive to combined treatment, p53-null MCF7 cells remained sensitive, albeit to a lesser degree (Figs. 5F–I).

To confirm that Pep8 sensitizes tumor cells to decreased levels of survivin, we measured the levels of cleaved caspase 7 and PARP as well as cell viability in MCF7 cells transfected with survivin siRNA followed by Pep8 treatment. The extent of caspase 7 and PARP cleavage is known to correlate well with the extent of apoptotic response (40). We showed that Pep8 cooperated with knockdown of survivin to induce apoptosis in both wild type and p53-null MCF7 cells (Suppl. Figs. 5D–E). We also showed that Pep8 cooperated with knockdown of survivin to decrease cell viability in MCF7 spheroids (Suppl. Figs. 5F–G).

Pep8 sensitizes MCF7 and HCT116 cells to YM155-induced DNA damage in a Rbm38-dependent manner

Increasing reports indicate that YM155 not only inhibits survivin expression but also elicits other cytotoxic effects, including DNA damage (41–43). As Pep8 cooperates with doxorubicin, a topoisomerase II (top-II) inhibitor, to induce DNA damage and growth suppression (7), we speculated that Pep8 may enhance YM155-induced DNA damage and apoptotic cell death. To that end, DNA damage was determined by measuring γH2AX, and apoptosis by measuring the levels of cleaved Caspase 7 and cleaved PARP in isogenic control, Rbm38-null, and p53-null MCF7 cells treated with Pep8 and YM155 alone or in combination. γH2AX was slightly increased in cells treated with Pep8 or YM155 alone (Figs. 6A–C, compare lane 1 with 2–3, respectively). However, concomitant treatment resulted in robust γH2AX accumulation in isogenic control, but not in Rbm38-null MCF7 cells (Figs. 6A–B). Further, concomitant treatment resulted in robust γH2AX accumulation in p53-null cells (Fig. 6C), which is consistent with a previous study that YM155 induces

DNA damage independent of p53 (43). Additionally, concomitant treatment with Pep8 and YM155 resulted in an enhanced apoptotic response in isogenic control and p53-null cells, but not in Rbm38-null cells (Figs. 6A–C). Similar results were observed with HCT116 cells treated with Pep8 and YM155 alone or in combination (Suppl. Figs. 6A–C).

While YM155-mediated γH2AX expression can be detected by western blotting, we questioned whether the assay is sensitive enough to determine subtle or localized increases in γH2AX as previously reported (44). To circumvent this, the number of γH2AX foci was measured by immunofluorescence staining. Indeed, we showed that YM155, but not Pep8, significantly enhanced the number of γH2AX foci in isogenic control and Rbm38-null MCF7 cells (Figs 6D–G). Nevertheless, we showed that the number of γH2AX foci was further increased by concomitant treatment with Pep8 and YM155 in isogenic control but not Rbm38-null MCF7 cells (Figs. 6D–G), consistent with the observation that Pep8 cooperates with YM155 to enhance γH2AX and growth suppression in a Rbm38-dependent manner. Since the mechanism by which YM155 induces DNA damage remains uncertain (41), we asked if Pep8 enhances etoposide-induced DNA damage, which has a well-defined mode of action as an inhibitor of topoisomerase II (45). Concomitant treatment with Pep8 and etoposide resulted in both an increase in the level of γH2AX protein and in the number of γH2AX foci in isogenic control cells (Suppl. Figs. 7A, D–E), but to a much lesser extent in Rbm38-null MCF7 cells (Suppl. Figs. 7B, F–G). Finally, we showed that the level of γH2AX was slightly increased in p53-null MCF7 cells treated etoposide alone and together with Pep8 (Suppl. Fig. 7C), highlighting the necessity of p53 for etoposide-induced, but not YM155-induced DNA damage.

Discussion

In this study, we demonstrated that Rbm38 not only increases, but also decreases survivin expression via two distinct pathways (Fig. 7). Mechanistically, Rbm38 impedes let-7b binding to survivin 3′-UTR (Fig 1L) and consequently, suppresses the ability of let-7b to decrease survivin expression (Fig. 1I and Suppl. Fig 1H). In contrast, Rbm38 directly interacts with Ago2 and promotes miR-203a-mediated degradation of survivin mRNA. However, Rbm38 ultimately enhances survivin expression by limiting let-7b accessibility, which is expressed at a 7-fold higher level than miR-203a in HCT116 and MCF7 cells (Fig. 2G). Thus, the relative abundance of these miRNAs can dictate the ability of Rbm38 to regulate survivin expression: increasing via high let-7b or decreasing via high miR-203a. Let-7b is typically viewed as a potent tumor suppressor since its expression is frequently decreased in cancers and serves as a prognostic marker (46). Interestingly, miR-203a expression is also decreased in a multitude of cancers (47), which would increase survivin. Therefore, in a tumor with decreased expression of let-7b and miR-203a, survivin would be further elevated by overexpression of Rbm38, which warrants further investigation. While the let-7 family encodes 9 mature miRNA, let-7b is the only member known to regulate survivin (48). However, it remains possible that other family members can regulate survivin and/or be regulated by Rbm38, which necessitates further investigation.

Pep8 was found to be docked in a pocket in the N-terminal domain of Ago2, where the key contact residues are negatively charged Glu-73 and/or Glu-76 (Fig. 3). Pep8 binds to Ago2

and disrupts the Ago2-Rbm38 complex as it does to the eIF4E-Rbm38 complex (7). As a result, Pep8 increases survivin expression by preventing miR-203a from degrading survivin mRNA (Fig. 4). Giving the high degree of flexibility of Ago2 N-terminal domain (Suppl. Fig. 3) and the regulation by Pep8, we question whether the Ago2 protein structure and function can be modulated through its interaction with Rbm38. Going further, it would be fruitful to determine if the Rbm38-Ago2 axis regulates other miRNAs that bind to survivin 3′-UTR.

Pep8 has previously been shown to induce p53 expression and enhance doxorubicin-mediated growth suppression (7). As increased survivin plays a role in chemo-/radio-resistance (19,20), we tested whether Pep8-mediated enhancement of survivin can be thwarted by YM155, a well-defined survivin inhibitor (37). We found that YM155 abrogates induction of survivin by Pep8, enhances apoptosis and cooperates with Pep8 to decrease the viability of spheroid cultures (Figs. 5–6, Suppl. Figs. 5–6). While Pep8 is known to induce growth suppression in Rbm38-/p53-dependent manners (7), we showed that p53-null cells remained highly sensitive to the combined treatment with Pep8 and YM155 (Figs. 5–6 and Suppl. Figs. 5–6). These data are consistent with our earlier observations that a combined treatment of Pep8 with doxorubicin is potent to induce growth suppression in p53-null cells (7). Since doxorubicin and YM155 can induce DNA damage, we questioned whether Pep8 sensitizes tumor cells to YM155-induced DNA damage. Indeed, Pep8 enhanced YM155-induced DNA damage in Rbm38-dependent but p53-independent manners (Fig. 6 and Suppl. Fig. 6). As combined treatment of Pep8 with etoposide was not able to enhance DNA damage in Rbm38-null or p53-null cells, our data support a previous study that YM155 induces DNA damage independent of p53 (43). The necessity for p53 in etoposide-induced DNA damage but not for that of YM155 may be due to their different modes of action. For example, etoposide inhibits DNA Top-II blocking DNA re-ligation leading to critical mistakes in DNA synthesis (45). In contrast, YM115 is shown to induce DNA damage via oxidative DNA cleavage upon 2-electron reductive activation (49). Nonetheless, further investigation is warranted to determine the mechanism(s) by which Pep8 enhances YM155-mediated DNA damage. As YM155 exhibit limited antitumor efficacy when used alone or in combination with other chemotherapeutic agents in Phase I-II clinical trials (50), Pep8 may be explored to sensitize tumors to YM155 treatment. Collectively, this study provides additional insight into the possibility that Pep8 may be explored as an adjuvant to sensitize tumors to DNA-damaging cancer therapeutic agents.

Supplementary Material

Refer to Web version on PubMed Central for supplementary material.

Acknowledgements

The authors would like to thank Chrisoula Toupadakis Skouritakis for creating the graphic working model. All simulations reported in this work were performed using the high-performance computational facilities at the NIH biowulf supercomputer. This project was funded in whole or in part with federal funds from the National Cancer Institute, National Institutes of Health, under contract HHSN261200800001E. The content of this publication does not necessarily reflect the views or policies of the Department of Health and Human Services, nor does mention of trade names, commercial products or organizations imply endorsement by the US Government. This research was

supported [in part] by the Intramural Research Program of NIH, National Cancer Institute, Center for Cancer Research.

Financial support: RO1 CA250338, RO1 CA195828, T32 CA108459, HHSN261200800001E

References

1. Lucchesi C, Zhang J, Chen X. Modulation of the p53 family network by RNA-binding proteins. Transl Cancer Res 2016;5. doi:10.21037/tcr.2016.08.30
2. Zhang J, Cho SJ, Shu L, Yan W, Guerrero T, Kent M et al. Translational repression of p53 by RNPC1, a p53 target overexpressed in lymphomas. Genes Dev 2011;25:1528–1543. [PubMed: 21764855]
3. Heinicke LA, Nabet B, Shen S, Jiang P, van Zalen S, Cieply B et al. The RNA Binding Protein RBM38 (RNPC1) Regulates Splicing during Late Erythroid Differentiation. PLoS One Published Online First: 2013. doi:10.1371/journal.pone.0078031
4. Chin K, DeVries S, Fridlyand J, Spellman PT, Roydasgupta R, Kuo WL et al. Genomic and transcriptional aberrations linked to breast cancer pathophysiologies. Cancer Cell 2006;10:529–541. [PubMed: 17157792]
5. Carvalho B, Postma C, Mongera S, Hopmans E, Diskin S, Van De Wiel MA et al. Multiple putative oncogenes at the chromosome 20q amplicon contribute to colorectal adenoma to carcinoma progression. Gut 2009;58:79–89. [PubMed: 18829976]
6. Hermsen M, Postma C, Baak J, Weiss M, Rapallo A, Sciutto A et al. Colorectal adenoma to carcinoma progression follows multiple pathways of chromosomal instability. Gastroenterology 2002;123:1109–1119. [PubMed: 12360473]
7. Lucchesi CA, Zhang J, Ma B, Chen M, Chen X. Disruption of the RBM38-eIF4E complex with a synthetic peptide PEP8 increases p53 expression. Cancer Res Published Online First: 2019. doi:10.1158/0008-5472.CAN-18-2209
8. Zhang Y, Feng X, Sun W, Zhang J, Chen X. Serine-195 phosphorylation in the RNA-binding protein Rbm38 increases p63 expression by modulating Rbm38's interaction with the Ago2–miR203 complex. J Biol Chem 2018;:jbc.RA118.005779.
9. Leveille N, Elkon R, Davalos V, Manoharan V, Hollingworth D, Oude Vrielink J et al. Selective inhibition of microRNA accessibility by RBM38 is required for p53 activity. Nat Commun 2011;2:513. [PubMed: 22027593]
10. Gebert LFR, MacRae IJ. Regulation of microRNA function in animals. Nat. Rev. Mol. Cell Biol 2019. doi:10.1038/s41580-018-0045-7
11. Paul P, Chakraborty A, Sarkar D, Langthasa M, Rahman M, Bari M et al. Interplay between miRNAs and human diseases. J. Cell. Physiol 2018. doi:10.1002/jcp.25854
12. Valencia-Sanchez MA, Liu J, Hannon GJ, Parker R. Control of translation and mRNA degradation by miRNAs and siRNAs. Genes Dev. 2006. doi:10.1101/gad.1399806
13. Friedman RC, Farh KKH, Burge CB, Bartel DP. Most mammalian mRNAs are conserved targets of microRNAs. Genome Res Published Online First: 2009. doi:10.1101/gr.082701.108
14. Höck J, Meister G. The Argonaute protein family. Genome Biol. 2008. doi:10.1186/gb-2008-9-2-210
15. Ye ZL, Jin HJ, Qian QJ. Argonaute 2: A novel rising star in cancer research. J. Cancer 2015. doi:10.7150/jca.11735
16. Bushati N, Cohen SM. microRNA Functions microRNA (miRNA): ~22-nt noncoding RNA that serves as a posttranscriptional regulator. Annu Rev Cell Dev Biol Published Online First: 2007. doi:10.1146/annurev.cellbio.23.090506.123406
17. Fabian MR, Sonenberg N, Filipowicz W. Regulation of mRNA Translation and Stability by microRNAs. Annu Rev Biochem Published Online First: 2010. doi:10.1146/annurev-biochem-060308-103103
18. Altieri DC. Survivin, cancer networks and pathway-directed drug discovery. Nat. Rev. Cancer 2008. doi:10.1038/nrc2293

19. Velculescu VE, Madden SL, Zhang L, Lash AE, Yu J, Rago C et al. Analysis of human transcriptomes [2]. Nat. Genet 1999. doi:10.1038/70487
20. Wheatley SP, Altieri DC. Survivin at a glance. J Cell Sci Published Online First: 2019. doi:10.1242/jcs.223826
21. Tang Z, Kang B, Li C, Chen T, Zhang Z. GEPIA2: an enhanced web server for large-scale expression profiling and interactive analysis. Nucleic Acids Res Published Online First: 2019. doi:10.1093/nar/gkz430
22. Krackhardt AM, Witzens M, Harig S, Stephen Hodi F, Jason Zauls A, Chessia M et al. Identification of tumor-associated antigens in chronic lymphocytic leukemia by SEREX. Blood Published Online First: 2002. doi:10.1182/blood-2002-02-0513
23. Dash S, Balasubramaniam M, Dash C, Pandhare J. Biotin-based pulldown assay to validate mRNA targets of cellular miRNAs. J Vis Exp Published Online First: 2018. doi:10.3791/57786
24. Dom G, Shaw-Jackson C, Matis C, Bouffioux O, Picard JJ, Prochiantz A et al. Cellular uptake of Antennapedia Penetratin peptides is a two-step process in which phase transfer precedes a tryptophan-dependent translocation. Nucleic Acids Res 2003;31:556–561. [PubMed: 12527762]
25. Zhang M, Xu E, Zhang J, Chen X. PPM1D phosphatase, a target of p53 and RBM38 RNA-binding protein, inhibits p53 mRNA translation via dephosphorylation of RBM38. Oncogene 2015;34:5900–5911. [PubMed: 25823026]
26. Phan N, Hong JJ, Tofig B, Mapua M, Elashoff D, Moatamed NA et al. A simple high-throughput approach identifies actionable drug sensitivities in patient-derived tumor organoids. Commun Biol Published Online First: 2019. doi:10.1038/s42003-019-0305-x
27. Goldman M, Craft B, Hastie M, Repečka K, McDade F, Kamath A et al. The UCSC Xena platform for public and private cancer genomics data visualization and interpretation. bioRxiv 2019;:326470.
28. Helwak A, Kudla G, Dudnakova T, Tollervey D. Mapping the human miRNA interactome by CLASH reveals frequent noncanonical binding. Cell Published Online First: 2013. doi:10.1016/j.cell.2013.03.043
29. Hoffman WH, Biade S, Zilfou JT, Chen J, Murphy M. Transcriptional repression of the anti-apoptotic survivin gene by wild type p53. J Biol Chem Published Online First: 2002. doi:10.1074/jbc.M106643200
30. Saleh AD, Savage JE, Cao L, Soule BP, Ly D, DeGraff W et al. Cellular stress induced alterations in microrna let-7a and let-7b expression are dependent on p53. PLoS One Published Online First: 2011. doi:10.1371/journal.pone.0024429
31. Zhang Y, Zhou SY, Yan HZ, Xu DD, Chen HX, Wang XY et al. MiR-203 inhibits proliferation and self-renewal of leukemia stem cells by targeting survivin and Bmi-1. Sci Rep Published Online First: 2016. doi:10.1038/srep19995
32. Zhang M, Zhang J, Chen X, Cho SJ, Chen X. Glycogen synthase kinase 3 promotes p53 mRNA translation via phosphorylation of RNPC1. Genes Dev 2013;27:2246–2258. [PubMed: 24142875]
33. Sheu-Gruttadauria J, Xiao Y, Gebert LF, MacRae IJ. Beyond the seed: structural basis for supplementary micro RNA targeting by human Argonaute2. EMBO J Published Online First: 2019. doi:10.15252/embj.2018101153
34. Elkayam E, Kuhn CD, Tocilj A, Haase AD, Greene EM, Hannon GJ et al. The structure of human argonaute-2 in complex with miR-20a. Cell Published Online First: 2012. doi:10.1016/j.cell.2012.05.017
35. Shimoda T, Ishida T, Suzuki S, Ohue M, Akiyama Y. MEGADOCK-GPU: Acceleration of protein-protein docking calculation on GPUs. In: 2013 ACM Conference on Bioinformatics, Computational Biology and Biomedical Informatics, ACM-BCB 2013. 2013 doi:10.1145/2506583.2506693
36. McKenna DJ, McDade SS, Patel D, McCance DJ. MicroRNA 203 Expression in Keratinocytes Is Dependent on Regulation of p53 Levels by E6. J Virol Published Online First: 2010. doi:10.1128/jvi.00703-10
37. Rauch A, Hennig D, Schäfer C, Wirth M, Marx C, Heinzel T et al. Survivin and YM155: How faithful is the liaison? Biochim. Biophys. Acta - Rev. Cancer 2014. doi:10.1016/j.bbcan.2014.01.003

38. Nunes AS, Barros AS, Costa EC, Moreira AF, Correia IJ. 3D tumor spheroids as in vitro models to mimic in vivo human solid tumors resistance to therapeutic drugs. Biotechnol. Bioeng 2019. doi:10.1002/bit.26845
39. Nakahara T, Kita A, Yamanaka K, Mori M, Amino N, Takeuchi M et al. Broad spectrum and potent antitumor activities of YM155, a novel small-molecule survivin suppressant, in a wide variety of human cancer cell lines and xenograft models. Cancer Sci Published Online First: 2011. doi:10.1111/j.1349-7006.2010.01834.x
40. Boucher D, Blais V, Denault JB. Caspase-7 uses an exosite to promote poly(ADP ribose) polymerase 1 proteolysis. Proc Natl Acad Sci U S A Published Online First: 2012. doi:10.1073/pnas.1200934109
41. Hong M, Ren MQ, Silva J, Paul A, Wilson WD, Schroeder C et al. YM155 inhibits topoisomerase function. Anticancer Drugs Published Online First: 2016. doi:10.1097/CAD.0000000000000441
42. Glaros TG, Stockwin LH, Mullendore ME, Smith B, Morrison BL, Newton DL. The 'survivin suppressants' NSC 80467 and YM155 induce a DNA damage response. Cancer Chemother Pharmacol Published Online First: 2012. doi:10.1007/s00280-012-1868-0
43. Chang BH, Johnson K, LaTocha D, Rowley JSJ, Bryant J, Burke R et al. YM155 potently kills acute lymphoblastic leukemia cells through activation of the DNA damage pathway. J Hematol Oncol Published Online First: 2015. doi:10.1186/s13045-015-0132-6
44. Ji J, Zhang Y, Redon CE, Reinhold WC, Chen AP, Fogli LK et al. Phosphorylated fraction of H2AX as a measurement for DNA damage in cancer cells and potential applications of a novel assay. PLoS One Published Online First: 2017. doi:10.1371/journal.pone.0171582
45. Montecucco A, Zanetta F, Biamonti G. Molecular mechanisms of etoposide. EXCLI J. 2015. doi:10.17179/excli2014-561
46. Balzeau J, Menezes MR, Cao S, Hagan JP. The LIN28/let-7 pathway in cancer. Front Genet 2017;8:31. [PubMed: 28400788]
47. Diao Y, Guo X, Jiang L, Wang G, Zhang C, Wan J et al. MiR-203, a tumor suppressor frequently down-regulated by promoter hypermethylation in rhabdomyosarcoma. J Biol Chem 2014;289:529–539. [PubMed: 24247238]
48. Chirshev E, Oberg KC, Ioffe YJ, Unternaehrer JJ. Let - 7 as biomarker, prognostic indicator, and therapy for precision medicine in cancer. Clin Transl Med Published Online First: 2019. doi:10.1186/s40169-019-0240-y
49. Wani TH, Surendran S, Jana A, Chakrabarty A, Chowdhury G. Quinone-Based Antitumor Agent Sepantronium Bromide (YM155) Causes Oxygen-Independent Redox-Activated Oxidative DNA Damage. Chem Res Toxicol 2018;31:612–618. [PubMed: 29897742]
50. Li F, Aljahdali I, Ling X. Cancer therapeutics using survivin BIRC5 as a target: What can we do after over two decades of study? J. Exp. Clin. Cancer Res 2019. doi:10.1186/s13046-019-1362-1

Significance

Findings show that Rbm38 exerts opposing effects on survivin expression via two miRNAs, and disruption of the Rbm38-Ago2 complex by an eight amino acid peptide sensitizes tumor spheroids to survivin inhibitor YM155.

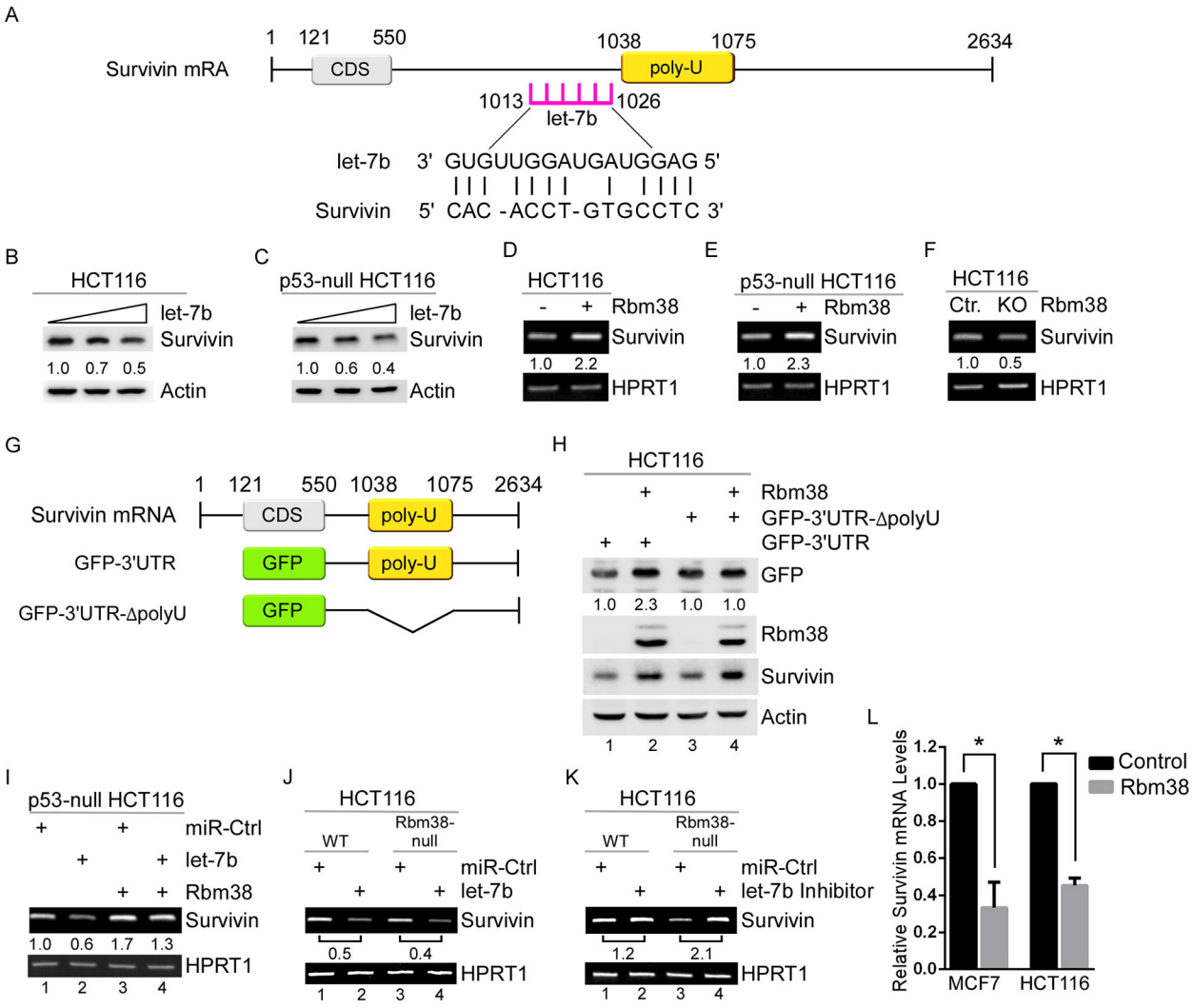

Figure 1. Rbm38 increases survivin expression by abrogating let-7b accessibility to survivin mRNA

A. Graphical representation of survivin mRNA and the binding region for let-7b.

B-C. Dose-dependent inhibition of survivin protein expression by let-7b (0 nM lane 1, 50 nM lane 2, and 100 nM lane 3) in WT (**B**) and p53-null HCT116 (**C**) cells.

D-E. RT-PCR analysis of survivin mRNA in WT (**D**) and p53-null HCT116 (**E**) cells uninduced or induced to express Rbm38.

F. RT-PCR analysis of survivin mRNA in isogenic control and Rbm38-null HCT116 cells.

G. Graphical representation of survivin 3'-UTR and GFP reporter constructs that contain a full-length or poly-U-deleted survivin 3'-UTR.

H. The levels of GFP, survivin, and Rbm38 proteins were measured in HCT116 cells transfected with a GFP reporter carrying a full-length or poly-U-deleted survivin 3'-UTR along with or without Rbm38 expression.

I. RT-PCR analysis of survivin mRNA in p53-null HCT116 cells transfected with a control or let-7b miRNA (100 nM) along with or without Rbm38 expression.

J-K. RT-PCR analysis of survivin mRNA in isogenic control and Rbm38-null HCT116 cells transfected with let-7b (100 nM) (**J**) or let-7b inhibitor (100 nM) (**K**).

L. qPCR analysis of survivin mRNA pulled down by 3' biotinylated locked nucleic acid (LNA) of miRNA let-7b mimic in MCF7 and HCT116 cells uninduced or induced to express Rbm38. (*P<0.05) Statistical analysis was performed by two-tailed unpaired t-test (mean ± standard deviation) (n=3).

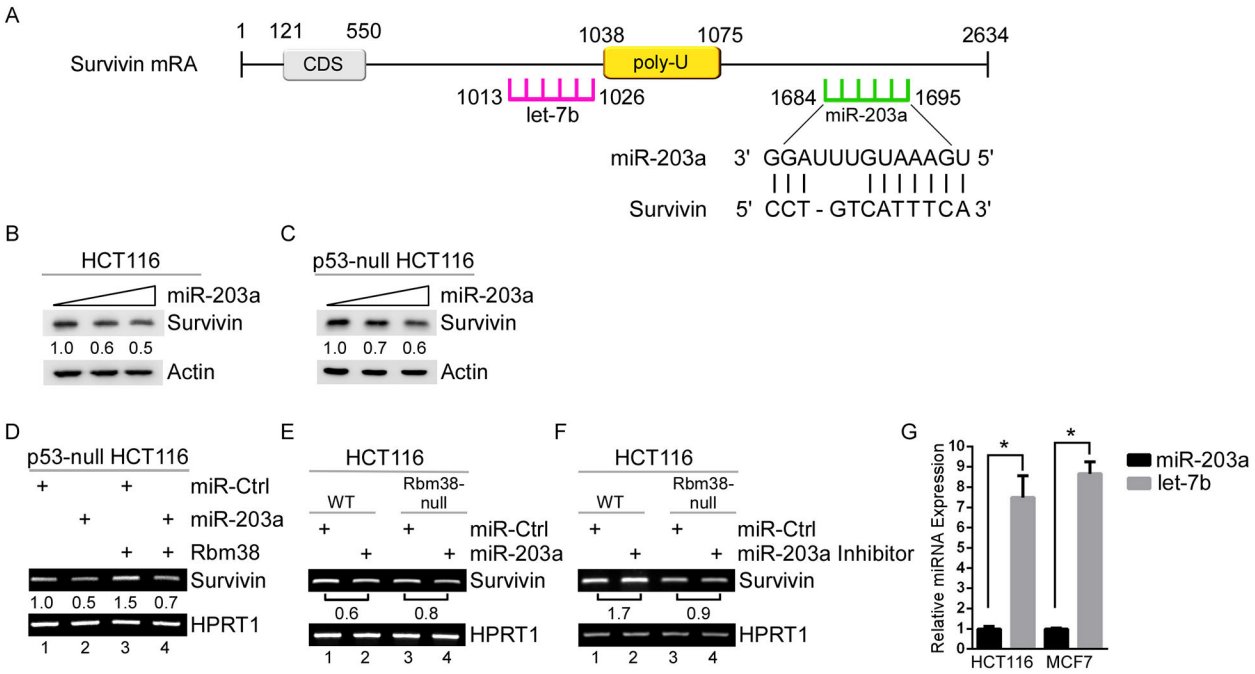

Figure 2. Rbm38 decreases survivin expression via miR-203a-mediated degradation of survivin mRNA.

A. Graphical representation of survivin mRNA and the binding regions for let-7b and miR-203a.

B-C. Dose-dependent inhibition of survivin protein expression by miR-203a (0 nM lane 1, 50 nM lane 2, and 100 nM lane 3) in WT (**B**) and p53-null HCT116 (**C**) cells.

D. RT-PCR analysis of survivin mRNA in p53-null HCT116 cells transfected with miR-203a (100 nM) along with or without Rbm38 expression.

E-F. RT-PCR analysis of survivin mRNA in isogenic control and Rbm38-null HCT116 cells transfected with miR-203a (100 nM) (**E**) or miR-203a inhibitor (100 nM) (**F**).

G. qPCR analysis of endogenous miR-203a and let-7b expression in HCT116 and MCF7 cells. (*P< 0.05) Statistical analysis was performed by two-tailed unpaired t-test (mean ± standard deviation) (n=3).

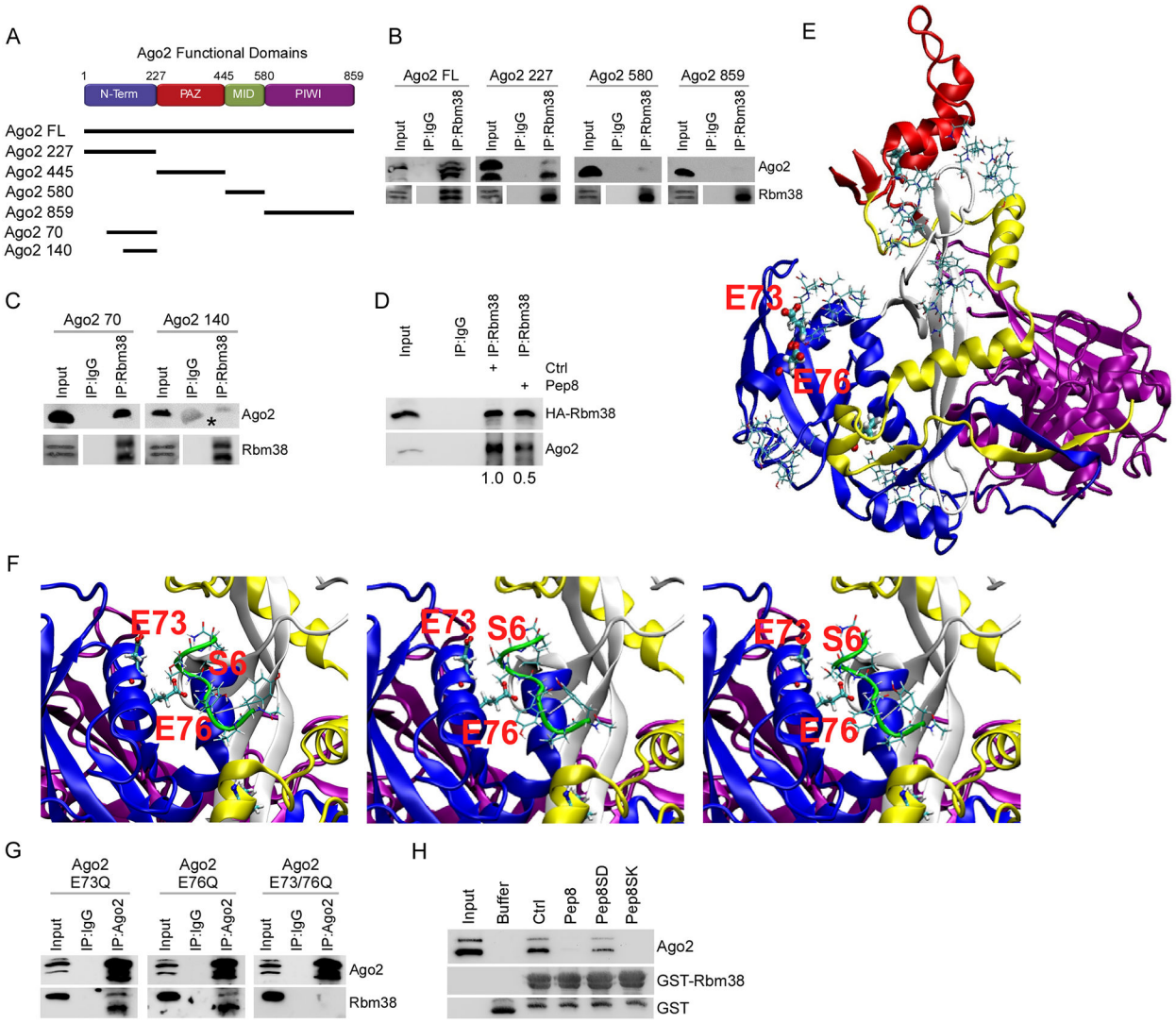

Figure 3. Ago2 interacts with Rbm38 via its N-terminal domain.

A. Graphical representation of Ago2 functional domains and Ago2-expressing constructs.

B-C. IP-western blot analysis was performed to measure the interaction of endogenous Rbm38 with the full-length Ago2 (**B**) or a fragment of Ago2 (**B-C**) ectopically expressed in MCF7 cells.

D. IP-western blot analysis was performed to measure the interaction of endogenous Ago2 with HA-tagged Rbm38 ectopically expressed in MCF7 cells in the presence of a control or Pep8 peptide (5 μM).

E. Visual representation of 6 selective potential Pep8-binding motifs on Ago2 protein.

F. Left panel – the most prominent binding mode between Pep8 and Ago2. Ser-6 of Pep8 forms a hydrogen bond with Glu-76 of Ago2. Middle and right panels - two alternative binding modes where Ser-6 of Pep8 is positioned between Glu-73 and Glu-76 of Ago2.

G. IP-western blot analysis was performed to measure the interaction of Ago2 227-E73Q, Ago2 227-E76Q, or Ago2 227-E73/76Q with Rbm38 ectopically expressed in MCF7 cells.

H. Competitive GST pull-down assay was performed to measure the interaction of recombinant Ago2 and GST-tagged Rbm38 in the presence of a control, Pep8, Pep8SD, or Pep8SK peptide (10 μM).

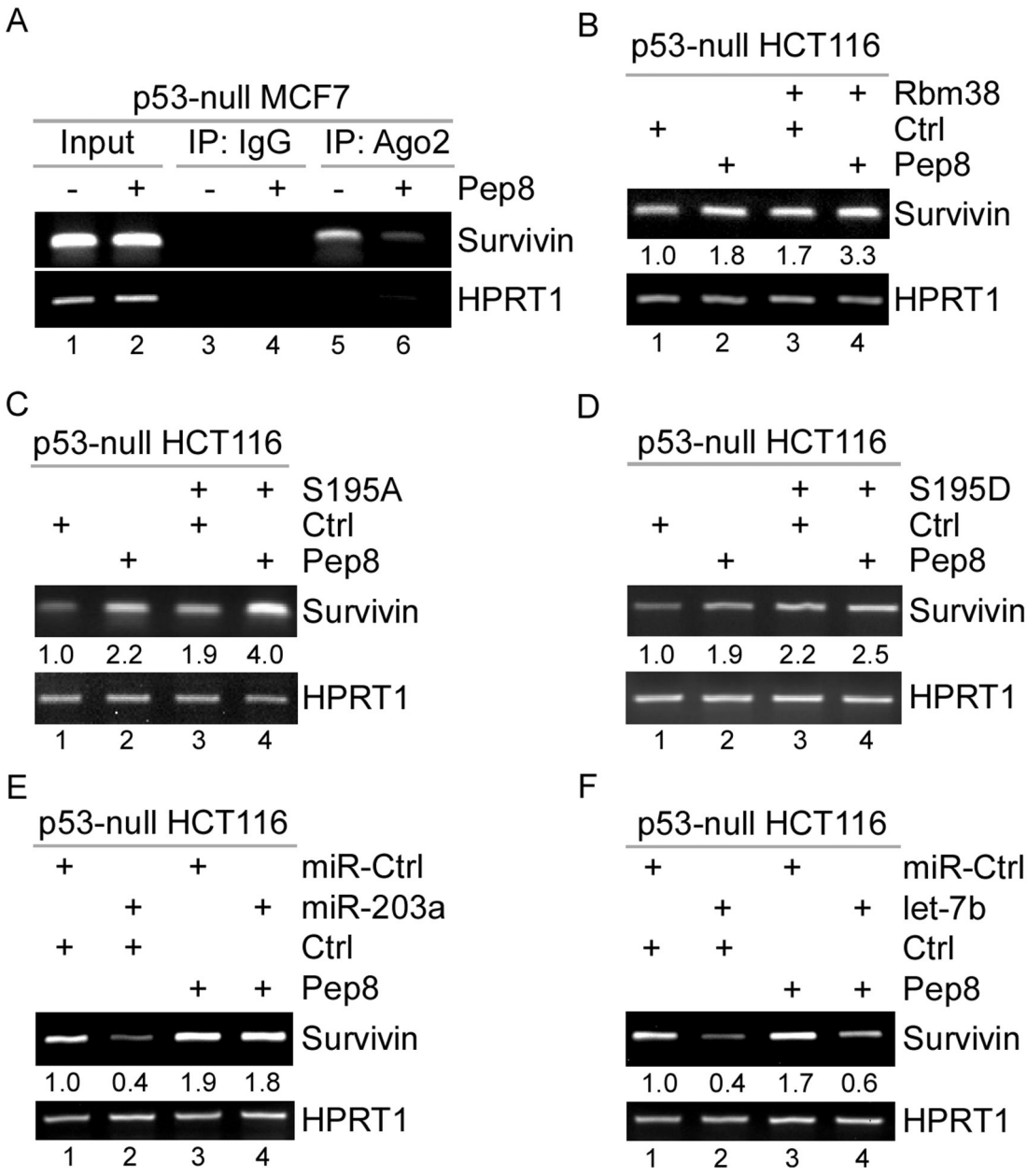

Figure 4. Pep8 abrogates the Rbm38-Ago2 complex to enhance survivin expression.

A. RNA-ChIP assay was performed to measure the binding of Ago2 to survivin mRNA in p53-null MCF7 cells treated with a control or Pep8 peptide (10 μM).

B. RT-PCR analysis of survivin mRNA in p53-null HCT116 transfected with a control or Rbm38-expressing vector along with treatment with a control or Pep8 peptide (10 μM).

C-D. RT-PCR analysis of survivin mRNA in p53-null HCT116 cells uninduced or induced to express Rbm38-S195A (**C**) or Rbm38-S195D (**D**) along with treatment with a control or Pep8 peptide (10 μM).

E-F. RT-PCR analysis of survivin mRNA in p53-null HCT116 transfected with miR-203a (100 nM) (**E**) or let-7b (100 nM) (**F**) along with treatment with a control or Pep8 peptide (10 μM).

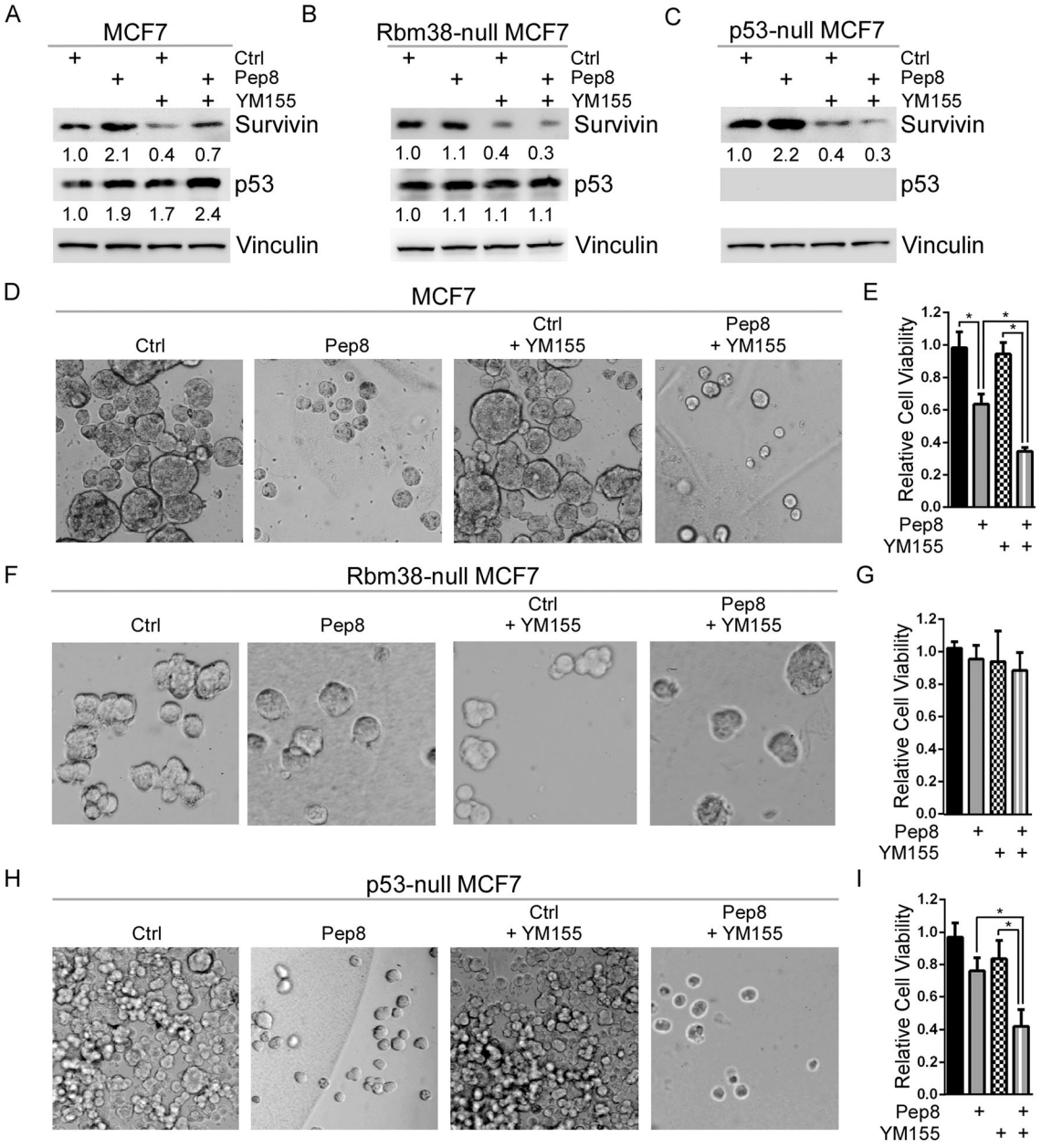

Figure 5. YM115 inhibits Pep8-mediated induction of survivin.

A-C. The levels of p53 and survivin protein were measured in MCF7 (**A**), Rbm38-null MCF7 (**B**), and p53-null MCF7 (**C**) cells treated with peptide alone (Ctrl or Pep8, 10 μM) or in combination with YM155 (3 nM) for 18 hours.

D-I. 3D spheroid cultures and relative cell viability were measured in MCF7 (**D-E**), Rbm38-null MCF7 (**F-G**), and p53-null MCF7 (**H-I**) cells after treatment with peptide alone (Ctrl or Pep8, 10 μM) or in combination with YM155 (3 nM) for 3 days. Spheroids were imaged with a 10x microscope objective. (*P< 0.05) Statistical analysis was performed by two-tailed unpaired t-test (mean ± standard deviation) (n=3).

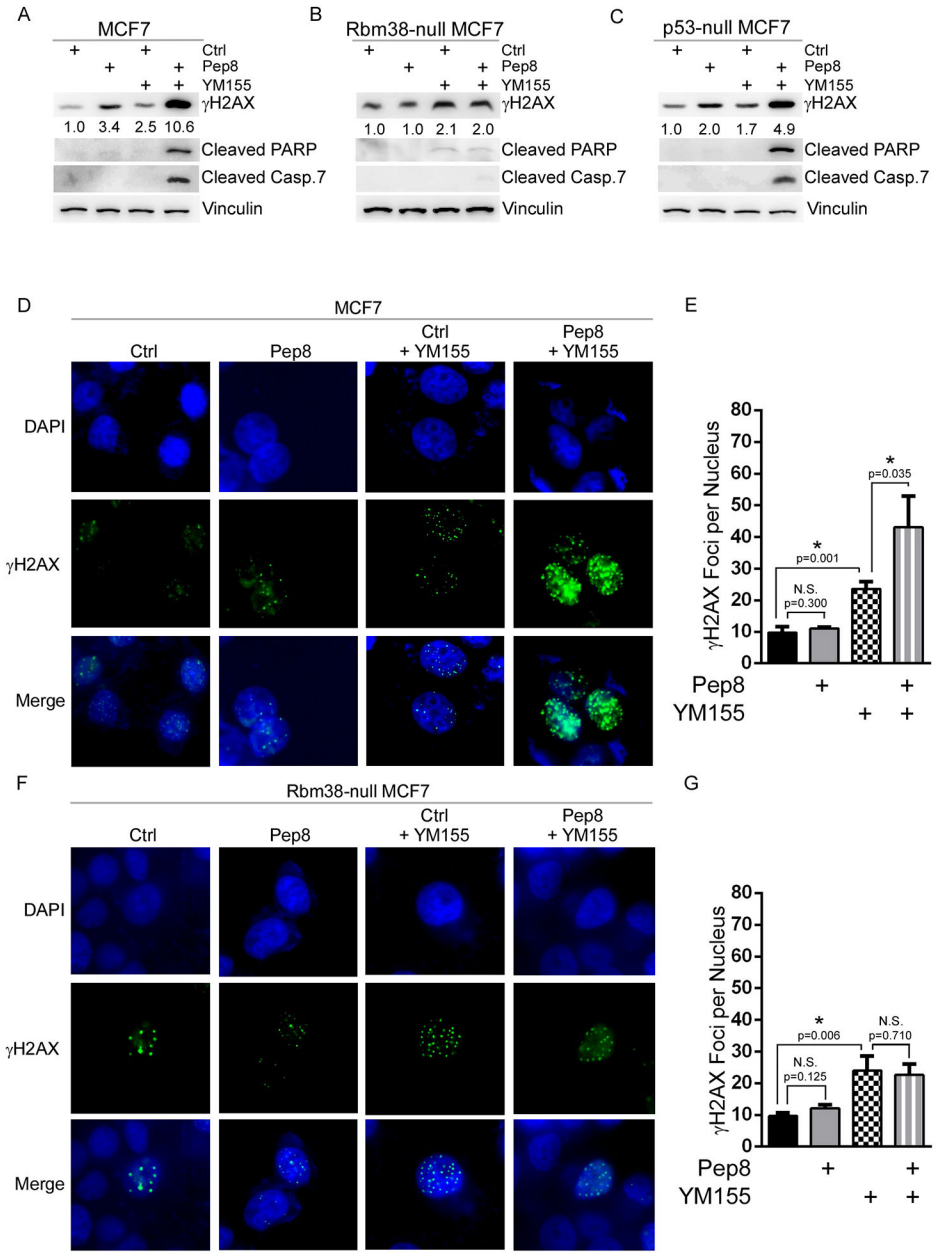

Figure 6. Concomitant treatment of Pep8 and YM155 induces γH2AX foci in an Rbm38-dependent manner.

A-C. Immunoblot for MCF7 (**A**), Rbm38-null MCF7 (**B**), and p53-null MCF7 (**C**) cells treated with peptide alone (Ctrl or Pep8, 10 μM) or in combination with YM155 (3 nM) for 18 h.

D-G. Representative immunfloursence images and number of γH2AX foci in isogenic control (**D-E**) and Rbm38-null MCF7 (**F-G**) cells treated with peptide alone (Ctrl or Pep8, 10 μM) or in combination with YM155 (3 nM) for 18 hours. Cells were imaged with a 63x microscope objective. (*P< 0.05) Statistical analysis was performed by two-tailed unpaired t-test (mean ± standard deviation) (n=3).

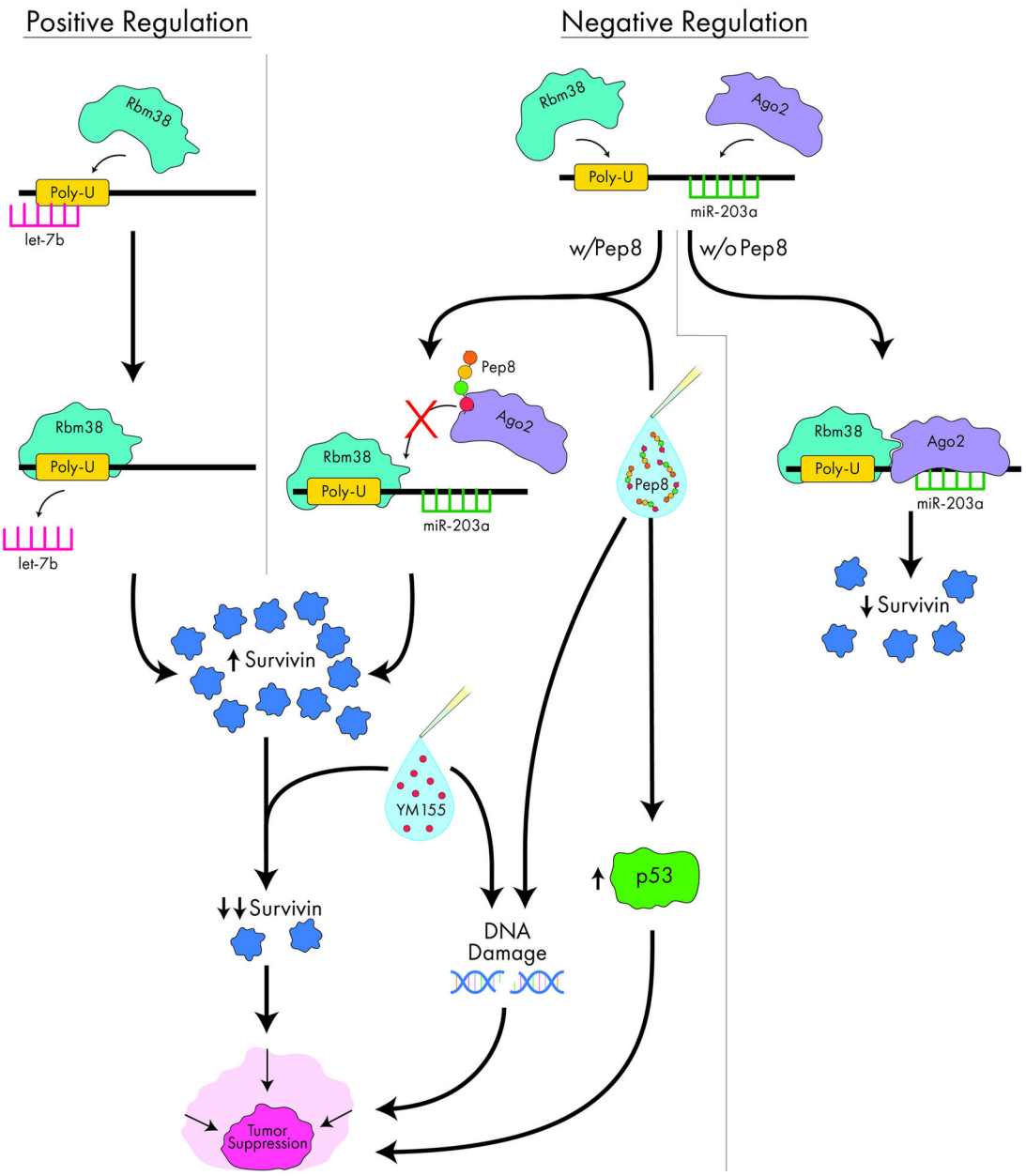

Figure 7:
A working model for how Rbm38 and Pep8 regulate survivin expression via miRNAs.